

Effective Ice Particle Densities for Cold Anvil Cirrus

Andrew J. Heymsfield, Carl G. Schmitt, and Aaron Bansemmer
National Center for Atmospheric Research
Boulder, Colorado 80301

Darrel Baumgardner
Universidad Nacional Autonoma de Mexico
04510 Mexico City, Mexico

Elliot M. Weinstock, and Jessica Smith
Harvard University
Cambridge, Mass.

Abstract. This study derives effective ice particle densities from data collected from the NASA WB-57F aircraft near the tops of anvils during the Cirrus Regional Study of Tropical Anvils and Cirrus Layers (CRYSTAL) Florida Area Cirrus Experiment (FACE) in southern Florida in July 2002. The effective density, defined as the ice particle mass divided by the volume of an equivalent diameter liquid sphere, is obtained for particle populations and single sizes containing mixed particle habits using measurements of condensed water content and particle size distributions.

The mean effective densities for populations decrease with increasing slopes of the gamma size distributions fitted to the size distributions. The population-mean densities range from near 0.91 g m^{-3} to 0.15 g m^{-3} . Effective densities for single sizes obey a power-law with an exponent of about -0.55 , somewhat less steep than found from earlier studies. Our interpretations apply to samples where particle sizes are generally below $200\text{-}300 \text{ }\mu\text{m}$ in maximum dimension because of probe limitations.

1. Introduction

Better characterizations of ice cloud particle properties are needed to improve the representation of ice and radiation processes in mesoscale and climate models and to facilitate accurate retrievals of ice cloud properties from ground- and satellite-based remote sensors. This study focuses on a major underlying property of ice cloud particles, their masses (m) or a related property, their effective ice densities (ρ_e). Though knowledge of the density and from measurements or representations of ice particle size distributions (PSDs), many ice cloud bulk properties such as the ice water content (IWC), the ice-mass flux (precipitation rate), and the equivalent radar reflectivity, can be derived.

Three methods have been used in earlier studies to estimate m or ρ_e for individual ice particles or as a function of the particle maximum dimension (D). One method (1), comprising most earlier studies, involves collecting ice particles in oil to obtain their maximum dimension, then melting them to obtain their melted equivalent diameter and mass [Magono and Nakamura, 1965; Heymsfield, 1972; Locatelli and Hobbs, 1974]. These relationships have almost exclusively been derived for single particle habits (e.g., hexagonal plates), or single particle types (e.g., aggregates, graupel). Method (2) uses measured IWCs and measured PSDs from

airborne probes to evaluate or infer appropriate $m(D)$ relationships [Brown and Francis, 1995]. In method (3) if an ice crystal is one of the regular types of geometrical shapes or habits observed under certain situations in ice clouds, the projected cross-sectional particle area and an assumed bulk ice density (that accounts for hollows within crystals) is used to provide an indication of its effective density [Heymsfield et al., 2002A]. Analytic relationships between particle dimension and mass can then be derived.

This paper extends the method of estimating ice particle mass or density for single particles or sizes and habits to the broader, more realistic case, of deriving mean effective densities for ice particle ensembles containing single or mixed particle habits. We also derive $m(D)$ relationships. The methods and the data sets are described in Section 2. Results are presented in Section 3. The results are summarized and conclusions drawn in Section 4.

2. Methods and Measurements

This section describes the methods and data sets used in this study. A detailed examination of the error sources, including possible measurement errors and biases in the estimates of ρ_e , are also discussed.

2.1 Methods

The method used to calculate the population-mean effective density is quite simple in principal. Direct measurement of the IWC yields the number of grams of ice per cubic meter of air. The coincident PSDs as measured by airborne particle size spectrometer are used to derive a total spherical particle volume per unit volume of air (V). This involves assuming that the measured particle population are spheres, from which

$$V = \pi/6 \sum N_i D_i^3, \quad (1)$$

where N_i is the ice particle concentration per size bins i and D_i is the midpoint diameter of the size bin. The population-mean effective density ($\bar{\rho}_e$) is just IWC/V . This result can readily be shown to be correct from analytic considerations by assuming exponential or gamma-type PSDs, but is not shown here for brevity.

The ($\bar{\rho}_e$) values can be related to other properties of the PSDs. The most direct variable is the slope of the particle size distribution, λ , which can be found by fitting the N_i versus D_i measurements from the size spectrometers to a single gamma-type size distribution of the form

$$N(D) = N_0 D^\mu e^{-\lambda D}, \quad (2)$$

where $N(D)$ represents the concentration per unit volume per unit size, N_0 is the intercept parameter, and μ the dispersion. The moment matching method described in Heymsfield et al. [2002] and in references cited in that article can be used to find the coefficients for the gamma fits. The median mass diameter, D_m , can then be found analytically for a gamma distribution [Mitchell, 1991] from

$$D_m = (\varphi + 0.67) / \lambda. \quad (3)$$

2.2. Measurements

This study uses measurements obtained by the NASA WB-57F aircraft during CRYSTAL FACE in southern Florida in July 2002. The WB-57F sampled cirrus formed by two different processes: deep convection, and in-situ generation. This paper focuses on the anvils and related ice cloud produced in association with the deep convection.

Particle size distributions were measured with the Droplet Measurement Technologies (DMT) Cloud, Aerosol, and Precipitation Spectrometer (CAPS) probe. The Cloud and Aerosol Spectrometer (CAS) probe portion of the CAPS produces data in 20 unequally-sized diameter bins between about 0.3 and 75 μm [REFERENCE DARREL?], We use the data in sizes between 5 and 75 μm to eliminate the possibility of including aerosols. Nonetheless, the CAS concentrations in each bin are subject to overestimates due to ice particle breakup on the inlet of the probe, especially when particles above several hundred microns are present. Particle sizes may also be overestimated by the assumption that the CAS particles are spheres. The Cloud Imaging Probe (CIP) portion of the CAPS retains the essential ingredients of a Particle Measuring System (PMS) 2D-C type probe, but has 64 size bins that span the particle diameter range from 25 to 1600 μm .

Baumgardner et al. [xxxx] discusses the processing algorithms for the CAS portion of the CAPS. The data were processed in 10-sec intervals to obtain a statistically accurate sample. The techniques we used to process the CIP data are given in Heymsfield [2002]. The CIP data processing includes the technique used to reconstruct partially imaged particles by Heymsfield and Parrish [1978]. For each CIP data set, concentrations were derived in 19, non-equally spaced, size bins for each five seconds, or approximately 600 m of flight. The CAS and CIP data sets were merged to provide a single size distribution between 5 and 1600 μm for each 5-seconds of flight.

The Harvard Total Water Instrument (TWI) samples vapor and, if present, condensate through a 1 cm (inside diameter) isokinetic inlet. A heater evaporates the condensate within the transit time from the heater to a water vapor detector, about 60 milliseconds. The heater design is predicated on the need to completely vaporize spherical particles with diameters up to 50 μm . A laser located downstream of the water vapor detector senses particles that are larger than the upper size limit for complete vaporization. The total water vapor content of the ambient air is measured (Weinstock et al., 1994) and the difference in water vapor contents between the TWI and those from a similar water vapor instrument that does not sample the condensate yields the IWC.

3. Results

The effective densities of particle populations and for single particle sizes are characterized in this section using ice water content and particle size distribution data. Four WB-57F research flight days, 9, 11, 23, and 29 July, representing a total of 914 5-sec in-cloud data points are included in this study. Other days were omitted from this analysis either because of data quality

issues or because the sampling was conducted in non-convectively generated cirrus. This section first looks at particle probe and total water instrument errors to identify the subset of the in-cloud periods that will yield reliable effective density values.

The transit time through the TWI instrument is inadequate to completely vaporize particles with melted diameters larger than about 50 μm , even though larger particles are frequently observed in the data set. Brown and Francis [1995] showed that the relationship

$$m(D)_{\text{BF}}=0.00294D^{1.9}, \quad (4)$$

the subscript referring to Brown and Francis, represented the $m(D)$ relationship for populations of mixed particle types observed in the ice clouds they sampled. This relationship spanned a wide range of particle sizes, although there were few if any situations where the $m(D)_{\text{BF}}$ relationship could have been tested in sub-100 μm particle sizes. Nonetheless, this relationship would suggest that ice particles above 50 μm , which according to this relationship have a solid ice density, might be incompletely vaporized. To assess the portion of the data set where incomplete vaporization may be an issue, the IWCs calculated from the PSDs (over all sizes) using Eq. (4) relationship were related to the median mass diameter derived from Eq. (3). A value of $\phi=1.9$ is used in Eq. (3) from Eq. (4), although ϕ can range between 1.9 to 2.5 for non-graupel ice particle types. Changing ϕ over this range leads to unimportant variations in D_m . Figure 1 shows the IWC calculated from Eq. (4) and the measured PSDs to the measured IWC as a function of D_m . Beginning with a value of D_m of 50 μm where the TWI should completely vaporize particles, the IWC ratio increases progressively, then flattens at a ratio of about four. Although Eq. (4) may not apply perfectly to our data set (see latter part of this section), we can conclude from Fig. 1 that the measured IWCs are appreciably underestimated where $D_m > 200 \mu\text{m}$. We therefore do not use any data where this limit is exceeded, the net effect leading to a reduction in the number of acceptable 5-sec periods to 300.

A desirable outcome of this study would be the development of an effective density relationship that could be representative of a particle size distribution. Such a relationship could be used in modeling studies and remote sensing retrieval algorithms. Figure 2 shows the calculated particle ensemble mean densities ($\bar{\rho}_e$) as a function of λ for the accepted subset of data from the four WB-57F CRYSTAL cases. The symbols represent the median values for different groups of data sorted by λ . The asterisks represent the median values sampled for λ intervals of 75 cm^{-1} , and the line is a least squares fit to the median values given by ****CARL**** overline below

$$\rho_e=0.00030 \lambda^{1.32}. \quad (5)$$

Mass-dimension relations are important for converting size distributions to bulk properties (e.g., precipitation rate). The IWC has been derived using our binned size distributions and Eq. (4) from Brown and Francis [1995]. Fig. 3A compares these calculated IWC to the measured values. The data is represented in terms of λ to assess variations with size. The factor of 2-3 differences in measured and calculated IWC values suggests that the $m(D)$ relationship can be refined to better represent our data.

To find a refined $m(D)$ relationship, we vary the coefficient a and exponent b in the power-law relationship of the type used by Brown and Francis ($m=aD^b$) to find a “best” fit to the measured IWC. This involves using the measured (non-parameterized) size distributions and first varying b , between 1.7 to 2.7 in increments of 0.05, to find the IWC . This range represents the range of b values reported in the literature for various ice particle types. The a coefficient is first taken to the Brown and Francis value of 0.00294. The IWCs calculated from this (a, b) pair are then compared to the measured values. The ratio, $\bar{r} = IWC(\text{calculated})/IWC(\text{measured})$ is averaged for all of the data points. A new a coefficient is then taken to be $0.00294/(\bar{r})$. The b value that produced the lowest value of the standard deviation of (\bar{r}) yielded the best representation of the $m(D)$ relationship for all data points. The resulting relationship,

$$m(D)=0.0103D^{2.45}, (6)$$

produced the best fit to the data. Fig. 3b shows the results using the relationship developed with the technique described above. Overall, this new relationship produces very good results over a wide range of λ .

4. Summary and Conclusions

This study uses measured condensed water contents and particle size spectrometer measurements in cold cirrus anvils during CRYSTAL FACE to derive the mean effective ice particle densities for ice particle populations, and as a function of size within the population. This study extends earlier observations of ice particle densities and masses that have been obtained primarily at the ground and represent populations of tens of particles rather than hundreds of thousands or millions as in the present study. It has the added benefit of measurements made directly in the tops of anvils that are crucial for radiative transfer studies. Our results, though, are limited to situations where particles are smaller than several hundred microns.

Using the relationships developed between $(\bar{\rho}_v)$ and spectral slope λ , it is simply a matter of finding the volume of the particle population from the fitted PSD coefficients, which, when multiplied by $(\bar{\rho}_v)$, yield IWC. Ryan [2000] and Heymsfield et al. [2002] describe method to derive λ . From measured (binned) size distributions, the size-dependent $(\bar{\rho}_v)$ relationships can be used to derive IWC. Using this technique, improvements can be made to estimates of IWC from past data sets where direct measurements of IWC were unavailable.

Acknowledgments. The NASA CRYSTAL program through NASA-NSF agreement number W-10 supported this research, 024, Don Anderson program manager. The authors are indebted to the crew of the WB57-F aircraft for their outstanding efforts with the data collection.

References

Brown, P.R.A., and P. N. Francis, Improved measurements of the ice water content in cirrus using a total-water probe. *J. Atmos. Oceanic Technol.*, 12, 410-414, 1995.

- Heymsfield, A. J., Ice crystal terminal velocities. *J. Atmos. Sci.*, 29, 1348-1357, 1972.
- Heymsfield, A. J., and J. L. Parrish, A computational technique for increasing the effective sampling volume of the PMS 2-D particle size spectrometer. *J. Appl. Meteor.*, 17, 1566-1572, 1978.
- Heymsfield, A. J., and G. M. McFarquhar, On the high albedos of anvil cirrus in the tropical Pacific warm pool: Microphysical interpretations from CEPEX and from Kwajalein, Marshall Islands. *J. Atmos. Sci.*, 53, 2424-2451, 1996.
- Heymsfield, A. J., A. Bansemer, P. R. Field, S. L. Durden, J. Stith, J. E. Dye, W. Hall and T Grainger, Observations and parameterizations of particle size distributions in deep tropical cirrus and stratiform precipitating clouds: Results from in-situ observations in TRMM field campaigns. *J. Atmos. Sci.*, 59, 3457-3491, 2002.
- Locatelli, J. D., and P. V. Hobbs, Fall speeds and masses of solid precipitation particles. *J. Geophys. Res.*, 79, 2185-2197, 1974.
- Magono, C., and T. Nakamura, Aerodynamic studies of falling snowflakes. *J. Meteor. Soc. Japan*, 43, 139-147, 1965.
- Mitchell, D. L., Evolution of snow-size spectra in cyclonic storms. Part II: Deviations from the exponential form. *J. Atmos. Sci.*, 48, 1885-1899, 1991.
- Ryan, B. F., A bulk parameterization of the ice particle size distribution and the optical properties in ice clouds. *J. Atmos. Sci.*, 51, 1436-1451, 2000.
- Weinstock, E. M., et al. , New fast response photo fragment fluorescence hygrometer for use on the NASA ER-2 and the Perseus remotely piloted aircraft, *Rev. Sci. Instrum.* 65, 3544-54, 1994, 2000.

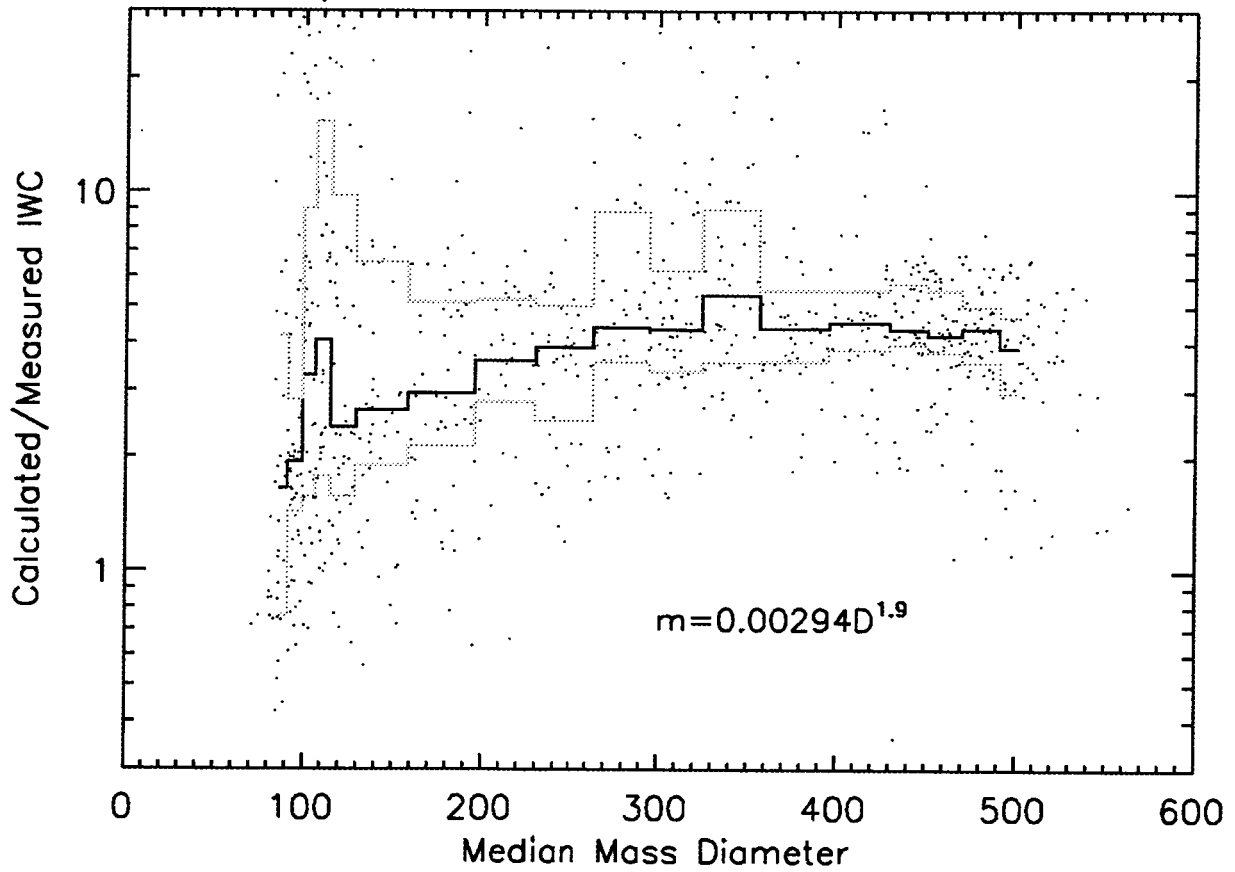
Figure Captions

Figure 1: For 914 in cloud data points, the ratio of the IWC calculated using Eq. (4) to the measured IWC, plotted versus the median mass diameter of the size distribution. Median values are shown with the bold line and the 25th and 75th percentiles are shown with the thin lines.

Figure 2: $(\overline{\rho_i})$ for the 300 accepted data points versus λ . The asterisks represent the median values for 75 cm⁻¹ intervals of λ . The solid line is a least squares fit to the median values.

Figure 3: A. The ratio of the IWC calculated using Eq. (4) to the measured IWC, plotted versus λ for the 300 point dataset. B. The ratio of ice water content calculated using Eq. (6) to the measured IWC, plotted versus λ . The median values are shown with the bold line and the 25th and 75th percentiles are shown with the thin lines on both plots.

Calculated/Measured IWC vs Median Mass Diameter



Particle Density vs λ

